THERMAL-HYDRAULIC ISSUES IN THE ITER TOROIDAL FIELD MODEL COIL (TFMC) TEST AND ANALYSIS

R. Zanino[a], M. Bagnasco[a], H. Fillunger[b], R. Heller[c], L. Savoldi Richard[a], M. Suesser[c] and G. Zahn[c]

[a] Dipartimento di Energetica, Politecnico, Torino, I-10129 Italy

[b] Atominstitut Wien, A-1020 Vienna Austria

[c] Forschungszentrum Karlsruhe, Institut für Technische Physik, D-76344 Eggenstein-Leopoldshafen Germany

ABSTRACT

The International Thermonuclear Experimental Reactor (ITER) Toroidal Field Model Coil (TFMC) was tested in the Toska facility of Forschungszentrum Karlsruhe during 2001 (standalone) and 2002 (in the background magnetic field of the LCT coil). The TFMC is a racetrack coil wound in five double pancakes on stainless steel radial plates using Nb_3Sn dual-channel cable-in-conduit conductor (CICC) with a thin circular SS jacket. The coil was cooled by supercritical helium in forced convection at nominal 4.5 K and 0.5 MPa. Instrumentation, all outside the coil, included voltage taps, pressure and temperature sensors, as well as flow meters. Additionally, differential pressure drop measurement was available on the two pancakes DP1.1 and DP1.2, equipped with heaters.

Two major thermal-hydraulic issues in the TFMC tests will be addressed here: 1) the pressure drop along heated pancakes and the comparison with friction factor correlations; 2) the quench initiation and propagation. Other thermal-hydraulic issues like heat generation and exchange in joints, radial plates, coil case, or the effects of the resistive heaters on the helium dynamics, have been already addressed elsewhere.

INTRODUCTION

Thermal-hydraulics has played a major role in the ITER TFMC [1] test and analysis. The two test campaigns of Phase I and of Phase II resulted in that a significant amount of ITER-relevant information, ranging from current sharing temperature to AC losses, could be extracted from the analysis of the TFMC performance. To make this possible,

CP710, *Advances in Cryogenic Engineering: Transactions of the Cryogenic Engineering Conference - CEC, Vol. 49,* edited by J. Waynert et al.

notwithstanding the fact that all diagnostics were located *outside* the coil, a suitable understanding of the thermal-hydraulics in the coil was needed [2-5].

Here we concentrate on a sub-set of specifically thermal-hydraulic issues of the TFMC test and analysis: 1) the analysis of the relation between pressure drop (Δp) and mass flow rate (dm/dt) in the different pancakes, particularly the ones equipped with heaters, where a dedicated differential pressure measurements was available (a first analysis of these data for Phase I was given in [6]); 2) a simple analysis of quench initiation and propagation in the coil (without making use of complex simulation tools). Other items of relevant thermal-hydraulic interest have already been considered elsewhere (e.g., the issue of heat generation and exchange in the joints [7, 8], or the above mentioned studies of the so-called safety discharge [4, 5], or the effects of the resistive heaters on the helium dynamics in the coil [9]).

CONSIDERATIONS ON THE TFMC-RELEVANT DATABASE FOR HELIUM FRICTION IN ITER CICC

The diagnostics available in the TFMC for this type of study consist of: temperature sensors with +/- 0.02 K accuracy at 5 K, flow meters with +/- 5 % accuracy with respect to the measured value (if the pressure head of the Venturi is larger than 10 mbar), and pressure drop transducers with an accuracy of ~ 1 % with respect to the maximum range of the transducer (which could be adjusted up to 1000 mbar). Between Phase I and Phase II, also in view of some inconsistencies noticed in the dm/dt measurements, the pressure drop transducers were recalibrated, but no obvious error was found. The existing TFMC-relevant database (to the best of our knowledge) is summarized in TABLE I.

Helium friction in an ITER CICC is customarily modeled (see, e.g., [8]) using one friction factor for each of the two main flow regions (see FIG 1):

1) The cable bundle region (considered, for the sake of simplicity, as a single region [1], i.e., the flow geometry defined by the wrappings is only taken into account in the definition of the wetted perimeter, flow area and void fraction) with friction coefficient f_B, for which the Katheder correlation [13] is often used;
2) The central channel (also called hole) with friction coefficient f_H, for which different more or less ad-hoc correlations exist, e.g., [14]-[16].

It is important to notice that, in order to have an independent verification of each friction factor correlation (i.e., of both f_B and f_H), two separate data sets are needed. Indeed, there are in principle infinite combinations of f_B and f_H able to reproduce the Δp vs. *total*

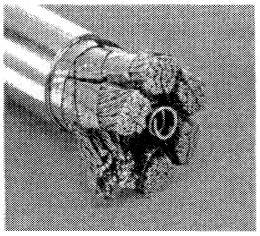

FIGURE 1. The TFMC conductor (outer diameter 40.5 mm). Notice the annular cable bundle region (void fraction ~ 36 %), with 6 last-but-one cabling stages (petals) delimited by wrappings, and the central channel (hole) region (inner diameter 10 mm), delimited by a 1 mm thick spiral.

[1] The only major exception to this, so far, is in the various attempts, see e.g. [10], [11], of explaining the reduced friction in the ITER Central Solenoid Insert Coil (CSIC) during operation with current by the occurrence of a third channel due to the deformation of the cable under electromechanical force. More generally, also the porous media nature of the bundle region has been recognized in, e.g., [12], [13], see below.

TABLE 1. TFMC-relevant database for helium friction in the CICC

	Fluid	Thermo-dynamic conditions	Comments
TFMC Phase I (FZK)	He / N_2	4.5 K, 0.6 MPa; RT ↔ 4.5 K	Global
TFMC Phase II (FZK)	He / N_2	4.5 K, 0.6 MPa; RT ↔ 4.5 K	Global
TFMC double pancakes (Ansaldo)	N_2	RT	Global
TFMC straight sample (CEA)	N_2	273 K, 3.0 MPa	Bundle, Global
3-turn TFMC sample (CEA)	N_2	273 K, 2.3-4.0 MPa	Global
TFMC spirals (CEA)	N_2	273 K	Hole
	H_2O	RT	Hole (forthcoming)
CSMC sample (CRPP)	H_2O	RT	Bundle, Global

dm/dt data of a CICC. Each of these, however, corresponds to a different flow repartition between the two regions. Since only one of these repartitions is correct, it is essential to have additional reliable data separately referring to either the bundle or the hole. Customarily, together with the (global) measurement of Δp, corresponding to the sum of the dm/dt in the bundle and in the hole, either of the following strategies has been adopted:

A. To separately measure the Δp corresponding to the dm/dt on the conductor in the bundle only (i.e., with the central channel blocked);

B. To separately measure the Δp corresponding to a given dm/dt in a pipe with rib-roughened internal wall in the form of an ITER spiral. It is then assumed that this will be the same as in the central channel of an actual ITER cable with the same spiral and the same $(dm/dt)_H$.

From TABLE 1 it appears that there are, for the TFMC, two independent means of verifying/deducing friction factor correlations and namely:

i) To use the data on the (5 m) TFMC straight sample and extract from these suitable f_B and f_H (this was done, but limited to the bundle region, in [17]), and/or

ii) To use the TFMC spiral data to deduce a correlation for f_H (as done, e.g., in [16]) and then use the TFMC data directly to deduce/verify f_B.

However, now that the TFMC tests have been completed, it is essential in our opinion to first of all start verifying the internal consistency of the database, also in order to get an assessment of the possible experimental error bars, before attempting the deduction of friction factors from those data. A first step in this direction is done in the following, for the global, bundle and hole data respectively.

Global data

In FIG 2 we plot a summary of the TFMC-relevant test results from TABLE 1. [2] The coordinates are $\langle\langle Re \rangle\rangle = (dm/dt)/\mu$ and $\langle\langle f \rangle\rangle = \frac{1}{2}\, \Delta p/L\, \rho/(dm/dt)^2$, proportional to the global Reynolds number and friction factor respectively (μ is the dynamic viscosity, L the sample or conductor length, ρ the density). This representation avoids ambiguities resulting from the different possible definitions of the total wetted perimeter and correspondingly of the total hydraulic diameter. Since the conductors have always the same cross section for all the data plotted, this is an acceptable representation and therefore, provided all the relevant physics is included in the hydrodynamic similarity, all of the data should fall on the same line, within error bars. However, while most of the data tend to fall on a single line, at least at large $\langle\langle Re \rangle\rangle$, where the measurement errors are expected to be smaller in relative terms, the data measured on the *straight* TFMC sample fall significantly below, see FIG 2. This was already noticed, to some extent, in [15], where it was argued that curvature effects might be

[2] For the TFMC we select two tests devoted to the measurement of Δp, without transport current, and namely those of Aug.1, 2001 (Phase I) and of Sep.12, 2002 (Phase II). In these tests, dm/dt was increased in steps allowing for a quasi steady state to be reached at each level. The temperature was kept constant between ~ 4.5 K and 4.65 K. The pressure varied because of the dm/dt regulation, but still kept in the range between about 4.8 bar and 6.1 bar.

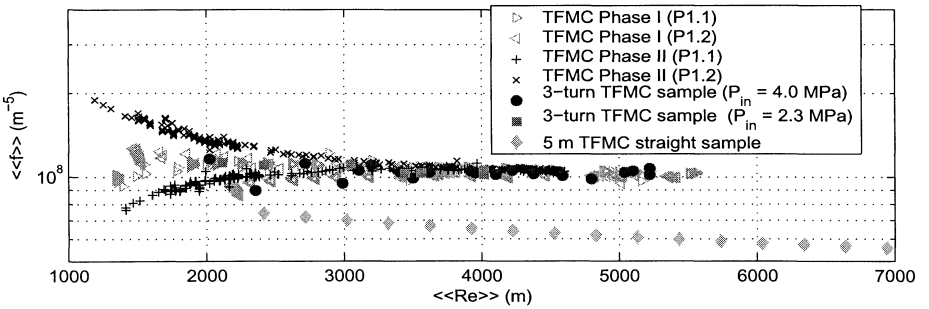

FIGURE 2. TFMC global "friction factor" <<f>> as a function of the global "Reynolds number" <<Re>> (see text for the definitions): a summary of available experimental data from the TFMC-relevant database.

responsible for the higher pressure gradient measured in the case of the 3-turn sample, if compared to the straight sample.

From an estimation of the curvature effect in the TFMC, according to [18], it turned out that only for the hole region the effect of curvature should be relevant. For the case of a smooth pipe, about 10% increase in the friction factor can be expected because of curvature, but it is not obvious how this generalizes to the actual case of a central channel with a spiral rib-roughened wall (roughness is known to enhance the effect of curvature on the Δp). If we further observe that only ~ 2/3 of the conductor trajectory in the TFMC is curved, it is not clear if one can attribute only to curvature the ~ 50% larger <<f>> reported in FIG 2 for the case of curved conductors.

Bundle region data

In TABLE 1 only two sets of bundle friction measurements are available up to now for ITER conductor samples. These are compared in FIG 3a. It is seen that the TFMC straight sample data [17] do not fall on the prolongation of the ITER Central Solenoid Model Coil (CSMC) sample data [19], but show a somewhat different trend as a function of Re_B. Notice that the only (hydraulic) difference between these two samples is their void fraction (~ 36.85% in the TFMC and ~ 36.3% in the CSMC), while the cabling differences appear to be negligible.

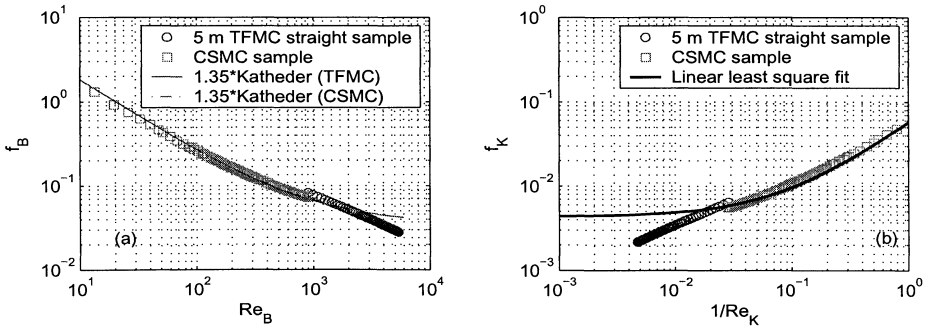

FIGURE 3. (a) Bundle friction factor f_B as a function of Re_B: experimental data (symbols) and results of Katheder correlation, multiplied by a factor of 1.35 (lines). (b) Friction factor f_K of the bundle, considered as a porous medium, as a function of $1/Re_K$: experimental data (symbols) and results of linear least square fit of all data.

In FIG 3a we also compare the prediction of a modified Katheder correlation, with multiplier 1.35, with the experimental data. This multiplier could be related, among others, to the swirling effect of wrappings (currently under evaluation based on data from Chinese conductors [20]). [3] While this allows a very good agreement with the CSMC sample data, it completely fails to reproduce the trend of the TFMC sample data.

A somewhat alternative approach to the problem of helium friction in the bundle region is reported in FIG 3b. Here the bundle is considered as an isotropic porous medium of permeability K (m^2), related to the strand diameter and to the bundle void fraction by the Carman-Kozeny relation [21]. Then $\sqrt{K}$ is used as scale length to define new friction factor and Reynolds number f_K and Re_K respectively. From first principles it is known (see, e.g., [21]) that the friction factor f_K should scale linearly with $1/Re_K$ (as verified in [12] for, e.g., the old NET conductor). If we attempt to least-square fit the *whole* data set (CSMC + TFMC sample data) linearly in $1/Re_K$, a very good agreement is obtained with the CSMC sample data (FIG 3b). On the contrary, much larger differences (up to a factor ~ 2) appear in the comparison with the TFMC sample data, which we cannot, at present, understand or explain.

Hole region data

In FIG 4 we finally concentrate on the friction data for the hole and their comparison with correlations. While both the CSMC and TFMC straight sample data were obtained by difference as explained above, the "spiral" data were directly measured on a rib-roughened pipe. It is seen from FIG 4 that the data from the TFMC straight sample and the spiral data are a factor of ~ 2 apart instead of falling on the same line, as they should in principle. The CSMC sample data are instead somewhat above the spiral (SHOWA) data, in view of the different g/h (gap/height) ratio (3 for the former vs. 2.8 for the latter).

If the correlation presented in [16] (deduced from the full spirals data set) is used with the appropriate g/h, it is seen that a very good agreement is obtained with the CSMC sample data, but obviously not with the TFMC straight sample data.

Summary on friction

- Global friction data may indicate some effect of curvature. Qualitatively, this should be relevant for the hole and irrelevant for the bundle, but quantitative assessment is difficult.
- TFMC and CSMC straight sample data for friction in the bundle region cannot be fully reconciled. Only the latter can be well reproduced with the Katheder correlation modified

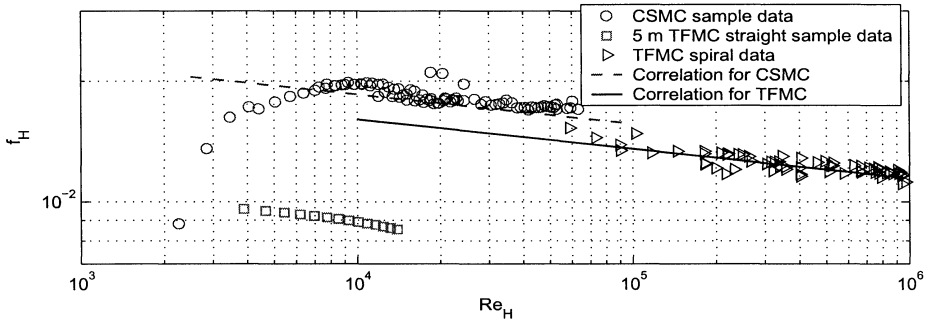

FIGURE 4. Hole friction factor as a function of Re_H: experimental data (symbols) and results of correlation from [16] (lines).

[3] The cabling pattern in general could also have effects on the friction in the bundle: it could be expected that, e.g., a shorter pitch of the various cabling stages could mean a more tortuous path for the helium and therefore somewhat higher friction.

with a suitable ad-hoc multiplier (1.35) or, alternatively, with theoretical correlations for friction in porous media.

- Hole friction data show an inconsistency between spiral data and TFMC straight sample. The correlation in [16] (deduced from spiral data) fits very well the CSMC sample. [4]
- The TFMC Phase I and Phase II data are reported in terms of $\Delta p/L$ in FIG 5. In view of the above-mentioned inconsistency, and of the good agreement between the correlation in [16] for f_H and the CSMC sample data, we use the same correlation for f_H for the analysis of the TFMC data, for the time being (i.e., until possible curvature effects have been quantified). Those data can then be fitted with very good agreement over a wide range of mass flow rates (see FIG 5) by using the Katheder correlation for the bundle friction with an ad-hoc multiplier, albeit much larger (~ 2.4) than for the CSMC sample. We cannot explain such a large multiplier (if any) from first principles, neither in relative terms to the CSMC nor in absolute terms. In principle, it could be related to a number of presently not quantified effects, as seen above: wrappings, conductor curvature, etc. From FIG 5 it is also clear, however, that the agreement between the present ITER design criteria (f_B deduced from the TFMC straight sample data, f_H from the spiral data) and the TFMC data can certainly be improved, and that the predictions of the design criteria are not conservative (actual pressure gradient underestimated by ~ 25%).
- As opposed to, e.g., the case of the CSIC or the CSMC, where a relatively large fraction of the conductor is at high field, and therefore subject to a high electromechanical load which could deform the cable [11], the peak field region in the TFMC is only 1-2 m long, i.e., much shorter than a pancake length (~ 70-80 m). It is therefore to be expected that operation with transport current should not significantly affect the hydraulic characteristic as it was confirmed, within error bars, during the tests (not shown).

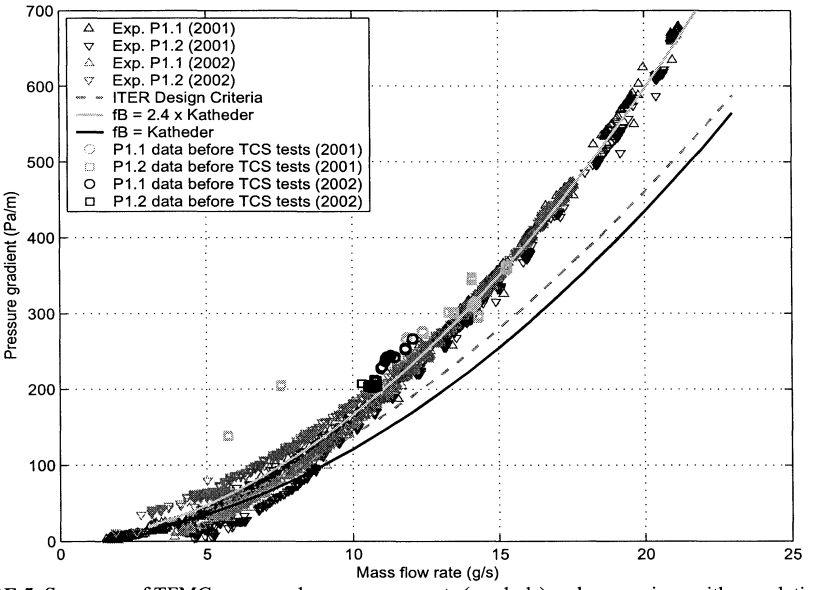

FIGURE 5. Summary of TFMC pressure drop measurements (symbols) and comparison with correlations (lines). As P11 and P12 use the same conductor, except for their length, it is to be expected that the pressure gradient $\Delta p/L$ should fall on the same line for both. The divergence of the curves below 10-12 g/s clearly indicates an increasing role of error bars at low dm/dt.

[4] Notice that the correlation in [16] for f_H, together with the Katheder correlation × 1.35 for f_B, also provide an excellent fit of the CSMC-1A data [22].

QUENCH INITIATION AND PROPAGATION IN THE TFMC P12 CONDUCTOR

During the TFMC tests, the Tcs measurements performed on conductor P12 sometimes initiated a quench in the coil. Resistive voltages were monitored both across the conductor (EK722 signal) and across the inlet joint (EDI712a and EDI712 signals, for the so-called short joint and long joint respectively, where the latter also includes a length $d_J \sim 0.6$ m of conductor on each side of the joint). The evolution of these signals is reported in FIG 6 for different transport currents in the TFMC.

From the comparison of the voltage take-off times in FIG 6a and FIG 6b it may be concluded that in all cases the quench is initiated in the conductor, and it reaches the joint region only after some tenths of second. The upstream quench propagation speed V_q^{up} can be estimated from the delay in the take-off of EDI712a (short joint) with respect to EDI712 (long joint) in FIG 6b. For the quench at 70/16 kA (the only one which occurred in the 2-coil operation), in TFMC and LCT coil respectively, the voltage take-off is towards negative (i.e., inductive) values, corresponding to the beginning of the current ramp-down (not shown). Indeed, in the 2-coil testing operation the peak magnetic field region where the quench is initiated is further from the joint compared to 1-coil testing, so that the quench does not reach the joint by up-stream propagation before the initiation of the safety discharge.

The total quench propagation speed can be estimated from the average slope of the EK722 signal as a function of time (see FIG 6a): considering the definition of the resistive voltage ($V_{EK722} = I\, \rho^{el}_{Cu}\, x_{norm} / A_{cu}$) and differentiating it with respect to time we have

$$\frac{\partial \rho^{el}_{Cu}}{\partial T}\frac{dT}{dt}\frac{x_{norm}}{A_{Cu}} I + \frac{\rho^{el}_{Cu} v_q}{A_{Cu}} I = \frac{dV_{EK722}}{dt} \qquad (1)$$

The first term in (1) can be neglected because T ~ 25-30K in the first tenths of second, so that $\frac{\partial \rho^{el}_{Cu}}{\partial T}$ is negligible (as confirmed by the quasi linear slope of $V_{EK722}(t)$).

The results of our analysis are summarized in TABLE 2. It may be noticed that the quench propagates somewhat faster down-stream than up-stream, and that both speeds tend

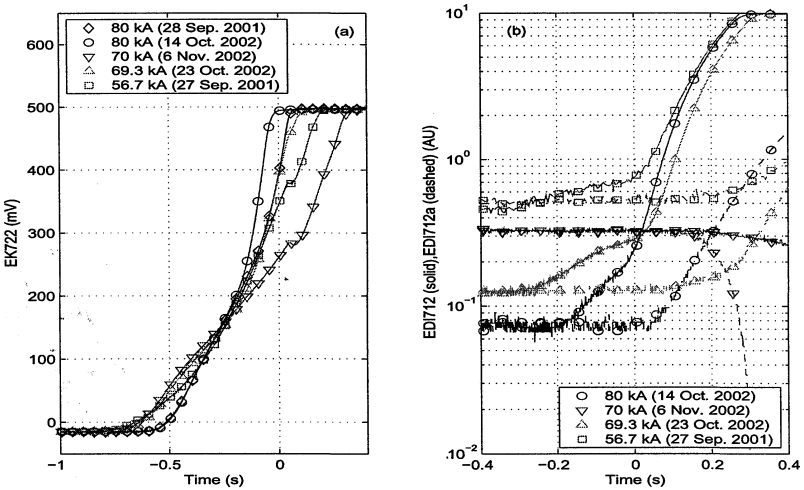

FIGURE 6. Measured evolution of voltage on P12 conductor (a) and inlet joint (b) during quenches at different currents. The time origin is set at the instant when the quench is detected (criterion 100 mV, 0.5 s delay). EDI712 and EDI712a have been base-lined to the same value for a given shot, but this value is arbitrary in order to make the figure more readable.

TABLE 2. Quench characteristics

	V_q (m/s)	V_q^{up} (m/s)	T_{max} (K)	p_{max} (bar)
80/0 kA (Oct.14, 2002)	6.7± 1	2.7± 0.3	37	9.0
70/16 kA (Nov.6, 2002)	5.0± 1	See text	30	12.5
69.3/0 kA (Oct.23, 2002)	5.0± 1	2.0± 0.2	49	9.0
56.6/0 kA (Sep.27, 2001)	3.6± 4.4	1.6± 0.1	39	9.0

to increase with the operating transport current, as expected. Also the peak temperature (TI712, at the P12 conductor inlet) and pressure (PI702) recorded in each case outside of the coil are reported, showing that the prompt reaction of the TFMC quench protection system allowed to keep them within tolerable limits.

CONCLUSIONS AND PERSPECTIVE

The analysis of the available TFMC-relevant database for helium friction in ITER CICC was presented. Some inconsistencies are present in the database, but TFMC Phase I and Phase II data can be reproduced using existing correlations for friction in the hole and ad-hoc modified correlations for friction in the bundle region. Although this may be sufficient for engineering purposes, some areas were identified where a more fundamental understanding of the coolant friction in ITER CICC is still lacking.

Quench initiation and propagation in the TFMC tests was analyzed by means of a simple model, aimed only at the assessment of the quench propagation speed. The data show no unexpected behavior. However, a more detailed and validated quench analysis in the ITER Model Coils, and in the TFMC in particular, is still an open problem. This could be needed for, e.g., the assessment of the hot-spot temperature by any of the existing sophisticated modeling tools for the analysis of thermal-hydraulic transients in superconducting coils, e.g., M&M [8].

REFERENCES

1. Libeyre, P., *et al.*, *IEEE Trans. Magn.* **32**, p. 2260 (1996).
2. Zanino, R., *et al.*, *Cryogenics* **43**, pp. 79-90 (2003).
3. Zanino, R., *et al.*, *Cryogenics* **43**, pp. 91-100 (2003).
4. Pasler, V., *et al.*, *Cryogenics* **43**, pp. 199-207(2003).
5. Nicollet, S., *et al.*, *Cryogenics* **43**, pp. 209-214 (2003).
6. Nicollet, S., *et al.*, *Proceedings* of the *19th ICEC*, pp. 161-164 (2002).
7. Zanino, R., *et al.*, *Proceedings* of the *18th ICEC*, pp. 363-366, (2000).
8. Savoldi, L., *et al.*, *Cryogenics* **40**, pp. 179-189 (2000).
9. Bagnasco, M., *et al.*, *Proceedings of XXI Congresso Nazionale sulla Trasmissione del Calore*, pp. 483-488 (2003).
10. Hamada, K., *et al.*, *Adv. Cryo. Eng.* **47**, pp. 407-414 (2002).
11. Zanino, R., *et al.*, *Adv. Cryo. Eng.* **47**, pp. 364-371 (2002).
12. Long, A., "Transverse heat transfer in a cable-in-conduit conductor with central cooling channel", Master of Science in Mechanical Engineering Thesis, MIT (1995).
13. Katheder, H., *Proceedings of the 15th ICEC*, pp. 595-598 (1995).
14. Hamada, K., *et al.*, *Adv. Cryo. Eng.* **43**, pp. 197-200 (1998).
15. Nicollet, S., *et al.*, , *IEEE Trans. App. Sup.* **10**, pp. 1102-1105 (2000).
16. Zanino, R., *et al.*, *IEEE Trans. Appl. Supercond.* **10**, pp. 1066-1069 (2000).
17. Nicollet, S., *et al.*, *Proceedings of the SOFT 98 conference*, pp. 771-774 (1998).
18. Rohsenow, W.M., Hartnett, J.P. and Garic, E.N., Eds., *Handbook of heat transfer fundamentals*, McGraw-Hill, New York, 1985.
19. Bruzzone, P., *Fus. Eng. Des.* **58-59**, pp. 211-215 (2001).
20. Weng, P.D. and Hongyu, B., Private communication (2003).
21. Nield, D.A. and Bejan, A., *Convection in porous media*, Springer, New York, 1998.
22. Savoldi Richard, L., *et al.*, *Proceedings of the 58° Congresso annuale dell'ATI* (2003) (in Italian).